

Experimental study of hydrogen pipeline leakage using rGO and Pd-NP decorated H₂-Sensors

Muti Adesina Adegboye^{1,2}, Bei Wang³, Jan Bickel³, James Njuguna^{1,2}, Ha Duong Ngo³

¹National Subsea Centre, 3 International Ave., Dyce,
Aberdeen, AB21 0BH, UK

²School of Engineering, Robert Gordon University, Garthdee Road,
Aberdeen, AB10 7QB, UK

³University of Applied Sciences Berlin, Treskowalle 8,
10318 Berlin, Germany

Abstract

The global interest in clean energy, such as hydrogen, spurred an interest in the use of the existing natural gas pipeline to transport hydrogen gas during the transition stage. However, leaks, which are the natural gas pipeline's main faults, could cause problems not only to the safety or environment but also offset some of the benefits of the hydrogen-related economy. Therefore, it is paramount to monitor pipelines for early leak detection to lower the risk of explosion. In this work, the feasibility of using advanced H₂ (Hydrogen) sensors for hydrogen pipeline leakage detections are conducted. An experiment was performed using rGO (reduced graphene oxide), rGO with Pd (Palladium) nanoparticle and rGO-Pd sputtering with the novel APSLD (Atmospheric Pressure Sputtering Layer Deposition) technology on IDE (Inter Digital Electrode) sensors attached to hydrogen flow rig. The relative response of the sensors to pipe leak size and H₂ concentration was measured by alternatively varying the pipe leak size and H₂/N₂ ratio. It was observed that these sensors' reaction to hydrogen gas could be used to detect hydrogen pipeline leakage. The rGO only sensor exhibited the highest relative response when it was exposed to H₂ gas. However, rGO with Pd nanoparticle and rGO-Pd sputtering with the APSLD sensors have rapid response/recovery time, which could be related to catalytic effect of Pd. Therefore, early detection of hydrogen leakage would be possible using the opportunity offered by advanced H₂ sensors, data collection and prognosis advancement.

Keywords: Hydrogen, Hydrogen leakage, Hydrogen sensor, Pipeline leakage, Reduced graphene oxide, Palladium nanoparticles

1. Introduction

Addressing climate change is a pivotal aspect of sustainable human development. One effective solution is enhancing the global energy share of non-polluting, renewable sources. As a clean energy type, hydrogen energy plays a critical role in reducing carbon emissions and serves as a vital energy storage medium, garnering increasing global interest. The efficient and safe transportation of hydrogen is thus a significant focus within

scientific and industrial sectors [1]. Europe, with its extensive natural gas pipeline network, can utilize existing facilities by connecting underground hydrogen storage and gas pipelines, effectively reducing transportation costs, accelerating deployment, and minimize environmental disruptions, thereby enhancing public acceptance. [2]. To mitigate the risk of hydrogen-related explosions, early detection of pipeline leaks is essential. Advances in hydrogen sensing technology based on nanomaterials provide new solutions for such monitoring [3-5]. In this work, we use sensors

made from modified reduced graphene oxide (rGO) and its composites with palladium (Pd) to enhance sensitivity and rapid response to hydrogen leaks. These rGO and Pd-based sensors demonstrate excellent performance under various hydrogen concentrations and pipeline leak sizes. Experimental data prove the feasibility and effectiveness of these sensors in detecting hydrogen leaks by varying the ratio of hydrogen to nitrogen and the size of the pipeline leaks. Specifically, the palladium deposition (APSLD) enhances the catalytic effect, further improving the response and recovery speed of the sensors.

2. Methodes

2.1 Preparation of hydrogen sensors

The sensors used in this study were developed using three material systems combined with standard MEMS (Micro-electromechanical Systems) technology and a 3D sputtering technique. The first material system is the rGO. rGO is available as a cheap nanomaterial with outstanding properties. HTW (Hochschule für Technik und Wirtschaft Berlin) developed a novel rGO deposition technique to deposit rGO onto IDE surfaces [6]. Using rGO as a sensing surface can further increase the total active surfaces for gas detection. The second material system is Pd. This material has the highest Hydrogen absorption and can change its phases due to Hydrogen concentration [3]. Pd is normally used in solid-state Hydrogen sensors. The electrical resistance of the rGO-Pd-Layer is a function of the Hydrogen concentration. The last material system is the Hydrogen foil from the NTT company. The IDE-sensor chips were fabricated vis standard MEMS technology using a glass wafer. First, a thin Ti/Au was deposited and patterned using wet etching. Followed by the realization of a passivation layer using BCB. The passivation layer is needed to functionalize the IDE surface with rGO and Pd. The schematic view and the manufactured IDE chips employed for studying hydrogen pipeline leakage are depicted in Fig. 1 and Fig. 2, respectively. The rGO and rGO+Pd were deposited on the IDE surfaces, and the rGO-chips realized are listed in Table 1.



Fig. 1, Schematic view of the IDE chips

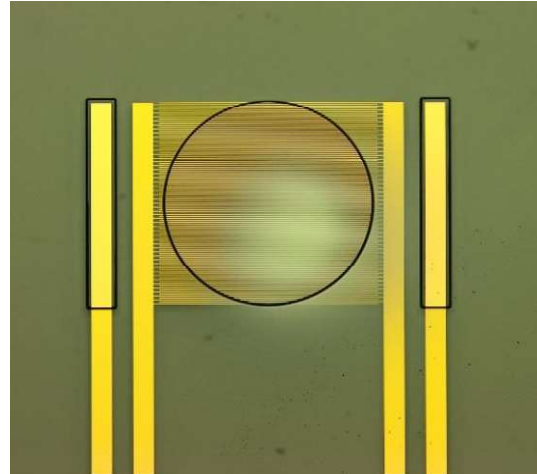


Fig. 2, Manufactured IDE-chip

Tab. 1: Chemical matrix for rGO-based sensors

Chip	Material	Process flow
IDE	rGO	Electro-phoretic HTW-rGO-deposition
IDE	rGO+Pd nanoparticle	Electro-phoretic HTW-rGO-deposition + dispensing NP Pd
IDE	rGO+Pd sputtering	Electro-phoretic HTW-rGO- deposition+deposition using HTW-APSLD

2.2 Experimental measurement

The experimentation of hydrogen pipeline leakage was carried out using a test rig constructed at the Robert Gordon University Aberdeen. Fig. 3 shows a schematic overview of the constructed experimental setup. The rig consists of (a) gas cylinders, (b) gas regulators, (c) mass flow controllers, (d) differential pressure transducer, (e) flow control valves, (f) flow meter, (g) hydrogen sensor, (h) testing chamber, and (i) Keysight U1241C multimeter data logger. The importance of detecting hydrogen gas leakage stems from its flammability and ability to explode in mixtures with air at a wide range of concentrations [7]. Accordingly, two cylinders were considered in the design of the experimental setup. One

cylinder for the hydrogen gas and the second for the nitrogen gas. Owing to the high flammability of pure hydrogen gas, the hydrogen cylinder was used to store a 10 % hydrogen and 90 % nitrogen gas mixture to provide a safe procedure for carrying out hydrogen experiments within the University environment. Pure nitrogen gas was then used to reduce the concentration of hydrogen gas from 10 % to the lower value. It is important to highlight that nitrogen was used in this study as a carrier gas to simulate the air.

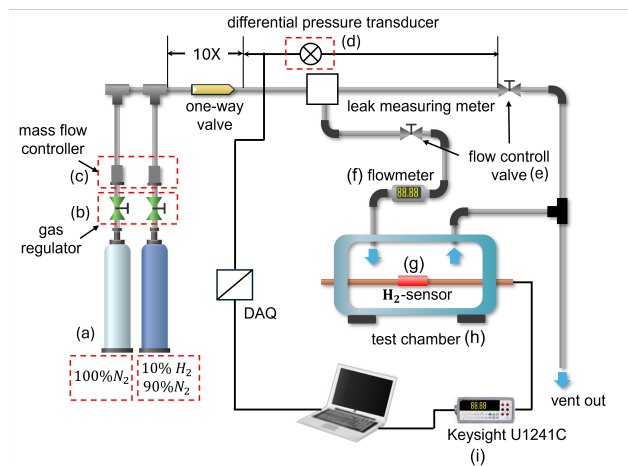


Fig. 3: Overview of the experimental setup for conducting hydrogen gas pipe leakage

The two cylinders were connected to the flow loop using BOC 8500 series hydrogen and nitrogen regulators to control and maintain accurate operating pressure in the system. The loop was designed to flow the defined hydrogen concentration by mixing pure nitrogen with a pre-mixed 10 % H₂ 90 % N₂ using two Omega mass controller systems (0 - 1 and 0 - 10 SLPM displays), which allowed to adjust the flow ratio of the hydrogen from 10% to 0.0001 % H₂ in standard liter per minute. The benefit of the setup is better control of the hydrogen concentration within the flow loop.

A pipe of 316/316L stainless steel with an internal diameter of 1/4 inches was used to ensure the system's maximum pressure of up to 58.6 MPa. To monitor the operating pressure in the testing section of the rig, a differential pressure (DP) transducer was introduced. The DP was mounted horizontally above the pipe for measuring the difference in pressure between the pipe upstream and

downstream. The gas response measurements were carried out using three different hydrogen sensors (rGO only, rGO+Pd nanoparticle and rGO+Pd sputtering technology) placed in a locally developed testing chamber. The testing chamber was designed to mimic the effects of environmental conditions the employed sensors may expose to during its usage. The chamber consists of input and output channels to allow a homogeneous mixture of nitrogen and hydrogen to flow in and out. It also provides a better setup for controlling the sensor's surface temperature. Other sensor's surround parameters can also be measured as the chamber can easily accommodate additional measurement devices such as temperature and humidity sensors. A silicon electric wire was attached to the sensor using electrically conductive epoxies (Chemtronics CW2400 Conductive Epoxy, 7g) and connected to Keysight U1241C multimeter for monitoring the sensing signal in the form of sensor resistance changes upon exposure to the hydrogen gas.

Keysight U1241C multimeter was used in this study to perform sensor's data recording and log the recorded data directly to the PC via a USB cable. The data logger can also record data into the main digital multimeter unit by using its built-in internal memory of up to 2,000 reading storage. Keysight U1241C multimeter measured and stored the sensor's output at a sampling of 1 to 200 kHz with an accuracy of 1 % + 5cnts. The measurement ranges were 0.1 Ω to 100 MΩ. The logger could also record the temperature and relative humidity from -40 to 1000 °C and 0 % to 80 % R.H, respectively. However, only the sensor's environment temperature was reported in this study. Pipe leakage testing procedures consisted of creating artificial leaks by partially opening the leak flow control valve (see Fig. 3) to control hydrogen flow into the chamber. The rate of hydrogen leakage in terms of the sensor's resistance changes during the leaking processes was recorded. The valve was closed after the sensor's resistance changes reached a stable state and recorded the sensor recovery time.

3 Results and discussion

3.1 Sensing properties of the hydrogen sensors

Three hydrogen sensors (rGO only, rGO+Pd nanoparticle and rGO+Pd sputtering) were used as sensing mechanics for the detection of hydrogen gas leakage. The sensing measurements were performed by measuring the changes in electrical resistance of the sensors as the sensors were alternatively exposed to hydrogen gas and air at 14.5 °C temperature. The sensing responses of sensors were measured after exposure to hydrogen gas. The sensing cycle was recorded in three steps: (1) continuous recording of sensor's resistance in the absence of hydrogen gas, (2) continuous flow of hydrogen gas (during the pipe leaking process) to record sensor's resistance changes, and (3) continuous recording of sensor's resistance in the air (after stopping leak discharge) to recover the sensors in their initial resistance value. The starting point of step (2) is considered the hydrogen leak state, while starting point of step (3) is regarded as an OFF state. One of the key parameters for evaluating the sensing characteristics of any gas sensor is the relative sensor response [8-10]. This work employed the relative response (SR) to evaluate the sensor's responses to the hydrogen gas. The sensor response is defined as the ratio of changes in sensor resistance in air and targeted gas:

$$SR(\%) = \frac{|R_a - R_g|}{R_a} \times 100\% \quad (1)$$

where R_g and R_a are the electrical resistance changes in detected gas and sensor resistance in the presence of air, the sensor response time was defined as the needed time for the sensor to reach 90 % signal maximum of hydrogen in the sensor environment. Together with the response time, the recovery time means the time needed to lower the signal maximum of 90 % [9].

Fig. 4 illustrates the dynamic response characteristic (relative response curve vs. time) for the three sensors measured at 5 % H₂ / 95 % N₂ mixture. The figures define two important parameters, i.e., the sensors' response time (T_{res}) and recovery time (T_{rec}). The time taken by the sensors to achieve 90 % of the total changes in relative response during the adsorption and desorption is known as the T_{res} and T_{rec} , respectively [8]. As shown in the results, good sensing characteristics were demonstrated in the three sensors. It took rGO based sensor 58 s to complete the reaction in the adsorption state and 76 s to return to its initial state by stopping the hydrogen injection (Fig. 4 (a)). Lower response (T_{res}) and recovery time were observed for the rGO+Pd nanoparticle and rGO+Pd sputtering-based sensors. The rGO+Pd nanoparticle-based sensor completed the adsorption reaction step

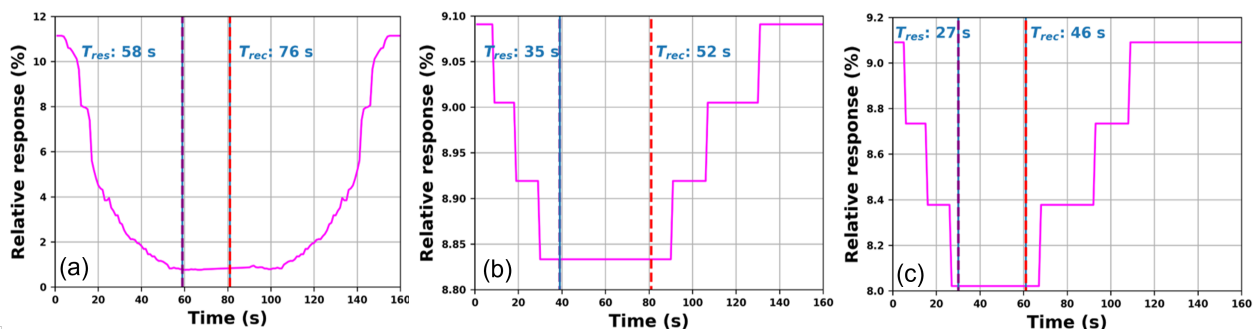


Fig. 4: Sensor's output based on hydrogen adsorption and desorption: (a) rGO only, (b) rGO+Pd nanoparticle and (c) rGO+Pd sputtering, response and recovery time comparison.

and returned to the original state, respectively, in 35 s and 52 s (Fig. 4 (b)), while the rGO+Pd sputtering-based sensor completed hydrogen adsorption and desorption in 27 s and 46s (Fig. 4 (c)), respectively.

Comparing the results of the three sensors, the rGO+Pd sputtering-based sensor has been demonstrated to respond rapidly to the hydrogen gas. While the rGO+Pd nanoparticle-based sensor was found to be faster than rGO only based sensor. Nevertheless, the response time of 58 s, 35 s and 27 s for the rGO only, rGO+Pd nanoparticle and the rGO+Pd sputtering, respectively, are satisfactory for studying hydrogen pipe leakage compared to other similar gas sensors [8, 12-14].

3.2 Analysis of sensor's output based on hydrogen concentrations

In addition to the sensor's response to the hydrogen gas, the three sensors' reactions to the different hydrogen concentrations ranging from 0.5 % to 5 % H₂ were investigated. The rig in Fig. 3 was designed to control the hydrogen concentration by changing the ratio of the hydrogen-nitrogen gases flow rate (10 % H₂ 90 % N₂) and high purity nitrogen (99.999%). The sensors response to the 0.5 %, 1 %, 2.5 % and 5 % hydrogen concentrations are depicted in Fig. 5. In all the sensors, the sensors responses result in resistance values increasing when exposed to the hydrogen gas.

A reversible decrease in resistance during the hydrogen off-stage was recorded. The SR of the three sensors (Fig. 5 (a), (b) and (c)) tends to increase with increased hydrogen concentration. It was observed that the SR of the rGO only based sensor increased and decreased linearly during the hydrogen ON stage and OFF stage. However, it took about 50 s to reach its maximum SR value. Contrary to the sensor's responses solely based on rGO (without palladium), the resistance of rGO+Pd nanoparticle and rGO+Pd sputtering based sensors increases and decreases in step stage manners (Fig. 5 (b) and (c)). The rGO+Pd sputtering based sensor reached its maximum SR value within 25 s, while the rGO+Pd nanoparticle sensor took about 35 s to attain its maximum SR value. Therefore, the unique properties of palladium nanoparticles and palladium sputtering materials play a crucial role in the tremendous enhancement of SR with fast response and recovery time, even at lower hydrogen concentrations, despite the fact that rGO sensor maintains high relative responses.

The fast response and recovery time of the rGO+Pd nanoparticle/ palladium sputtering based sensors at lower concentrations of hydrogen gas can be linked to the hydrogen interaction mechanism of the rGO+Pd interface [9]. It was established in [15] that adding palladium nanoparticle to rGO could improve the hydrogen sensor response/recovery time. It

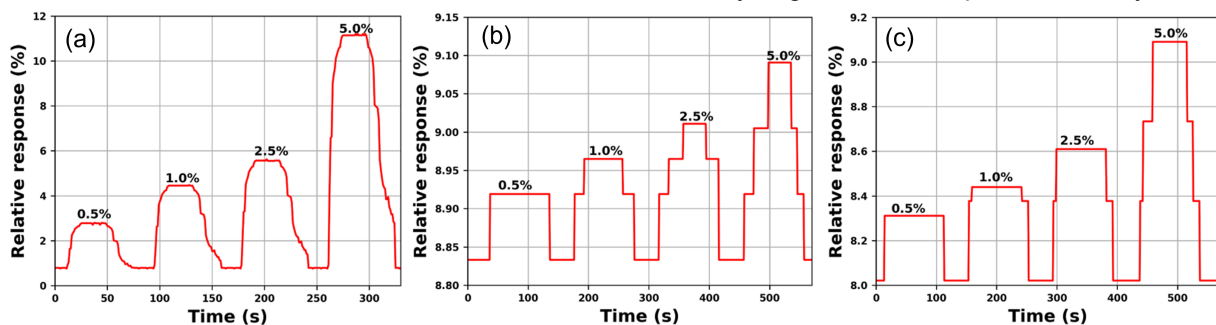


Fig. 5: The response-recovery curves of the different hydrogen concentrations: (a) rGO only, (b) rGO+Pd nanoparticle and (c) rGO+Pd NP + Pd sputtering.

is important to highlight that palladium itself is a sensing material for hydrogen sensor. However, adding palladium nanoparticles to the rGO can act as a catalyst to improve rGO

sensor conductance, response time, stability, and reversibility. The hydrogen sensing mechanism in palladium sensor is the result of the electronic effect, while the physical adsorption of hydrogen on the Pd surface caused the formation of Pd-hydride (PdH_x) [9]. Consequently, the sensing mechanism in rGO/Pd composite layers can be attributed to the (1) interaction of rGO and Pd and (2) effects of the hydrogen on the Pd and rGO interface. Therefore, it could be concluded that the response time and recovery time (Fig. 5 (b) and (c)) were improved by the presence of the palladium material in rGO.

Investigation of hysteresis characteristics of the hydrogen sensor for continuous use is essential to check if the sensor's measured performance is satisfactory and maintainable. Fig. 6 depicts four cycles of the three sensors ON and OFF state responses for 5% H_2 concentration. The results in Fig. 5 (a), (b) and (c) were repeated by sequentially exposing the sensors to 5% and 0% hydrogen concentrations to the signal outputs. The three sensors signal reactions to 0% and 5% hydrogen concentrations for four consecutive cycles were compared, and the output signals remained nearly unchanged in every hydrogen cycle, which demonstrates that these sensors preserve good repeatability.

The effect of hydrogen pipe opening size on the sensors' responses was investigated. The pipe leakage was created using a flow control valve (Fig. 3). Experimentation of pipe leakage for different leak sizes (0.1250, 0.0833 and 0.0625) corresponding to leak1, leak2 and leak3 are conducted and analyzed. Note that the leak sizes (0.1250, 0.0833 and 0.0625) are defined as the ratio of pipe opening size to pipe internal diameter. The changes in the electrical resistance of sensors were recorded as the pipe leak size was alternatively varied. The sensing cycle was recorded in three steps: (1) continuous recording of sensor's resistance in the absence of hydrogen gas, (2) continuous flow of hydrogen gas (during the pipe leaking process) to record the sensor's resistance changes, and (3) continuous recording of sensor's resistance in the air (after stopping leak discharge) to recover the sensors in their initial resistance value. The resulting sensors responses for leak1, leak2 and leak3 are shown in Fig.7. The sensor response profile in Fig.7 (a) illustrates obtained results for rGO based sensor, while Fig.7 (b) and Fig.7 (c) are respectively results of rGO+Pd nanoparticle and rGO+Pd sputtering based sensors. The results in Fig. 7(a) indicate that the magnitude of pipe opening size affects the rGO-based sensor responses. The increase in pipe leak size leads to the sensor's relative response increases. However, the reverse was observed in hydrogen leak detection time. As exemplified in Fig. 7(a), the higher the leak size, the lower

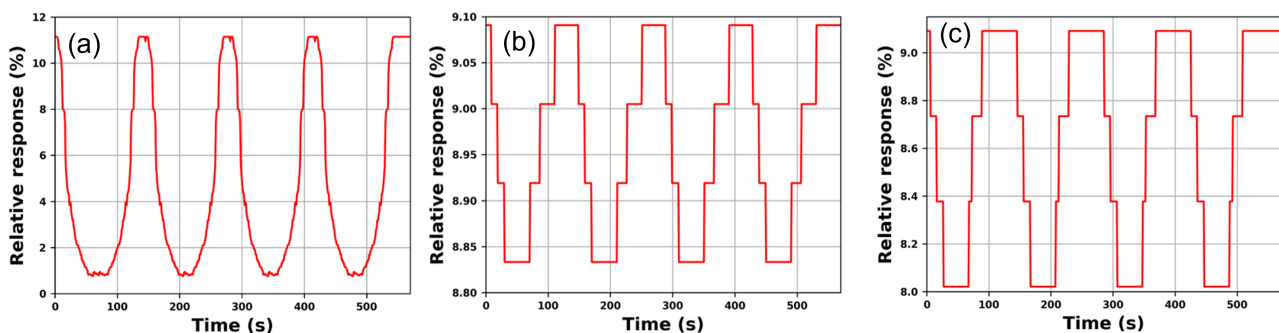


Fig. 6: Analysis of hysteresis characteristics outputs: (a) rGO only, (b) rGO+Pd nanoparticle and (c) rGO+Pd sputtering for four consecutive ON/OFF hydrogen cycles.

3.3 Effect of pipe opening size

time it takes to detect the occurrence of hydrogen leakage. A similar response was also observed for rGO+Pd nanoparticle and rGO+Pd sputtering-based sensors.

The hydrogen pipe leak size was investigated using 1 % and 5 % H₂ concentrations. The two concentration values were considered to cover nonexplosive and explosive hydrogen concentration ranges. The sensors response to

different leak sizes and H₂ concentration. The relative response of the sensors to the hydrogen was measured, and the time required to respond/recover was studied for explosive and nonexplosive hydrogen limits. The experiment results show that the relative response decreases with increased of hydrogen leak size. The results also revealed that the higher the hydrogen concentration, the more relative response increases.

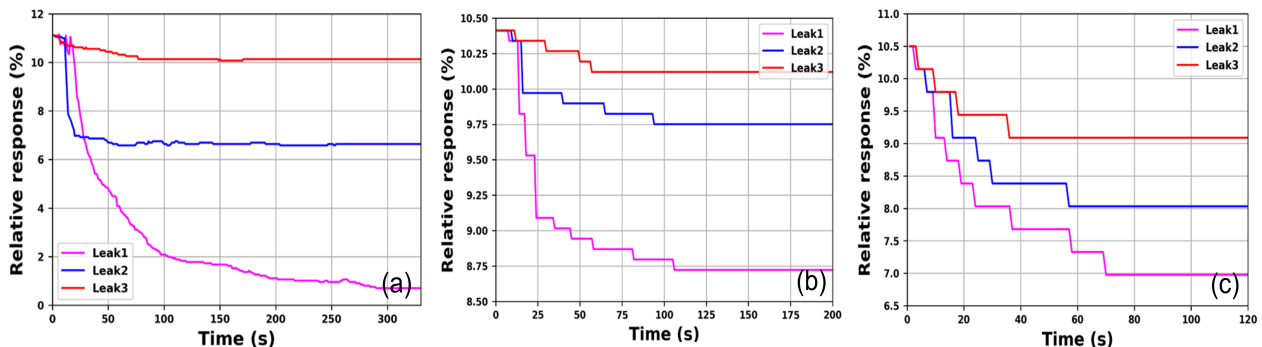


Fig. 7: Leak sizes variation sensors response; (a) rGO only, (b) rGO+Pd nanoparticle and (c) rGO+Pd sputtering.

the hydrogen leakage are varies based on pipe leak size and hydrogen concentration. For 1% H₂, the rGO only, rGO+Pd nanoparticle and rGO+Pd sputtering sensors response time to the smallest leak size (0.0625) are respectively 300 s, 110 s and 70 s, while the corresponding response time for the 5 % H₂ are 47 s, 36 s and 30 s. It was found that the sensors used in this work demonstrated fast response/recovery time [3]. Especially rGO+Pd nanoparticle and rGO+Pd sputtering-based sensors. This implies that incorporating any of these sensors into the hydrogen monitoring device could aid the quick information about the state of the hydrogen pipeline and early detection of hydrogen leakage.

4. Conclusion

In conclusion, the feasibility of detecting hydrogen pipeline leakage using an advanced H₂ sensor is proposed and experimentally demonstrated in this paper. A simple hydrogen flow rig had been constructed, and the sensing performance of rGO only, rGO+Pd nanoparticle and rGO+Pd Sputtering sensors attached to the flow rig investigated under

The response/recovery time of the rGO only, rGO+Pd Sputtering rGO+Pd nanoparticle sensors are respectively 300 s / 309 s, 110 s / 117 s and 70 s / 81 s for 1 % H₂, 0.0625 leak size. While the corresponding response/recovery time for 5 % H₂ are respectively 47 s / 60 s, 36 s / 43 s and 30 s / 38 s for rGO+Pd Sputtering and rGO+Pd Nanoparticle sensors. This implies the possibility of detecting hydrogen leakage in advance and lowering the risk of explosion.

Acknowledgement: Authors thank the Royal Society of Edinburgh for supporting this project through project no 43982.

References

- [1] Adoption of the G20 Japan. Report prepared by the IEA(International Energy Agency), June 2019, Available online: <https://www.iea.org/reports/the-future-of-hydrogen>
- [2] German National Hydrogen Council. Published by Nationaler Wasserstoffrat, 2.July.2021, Available online: <https://www.wasserstoffrat.de/fileadmin/wasserstoffr>

[at/media/Dokumente/EN/2021-07-02_NWR-Information Paper Hydrogen Transport.pdf#:~:text=URL%3A%20https%3A%2F%2Fwww.wasserstoffrat.de%2Ffileadmin%2Fwasserstoffrat%2Fmedia%2FDokumente%2FEN%2F2021](#)

[3] B. Wang, L. Sun, M. Schneider-Ramelow, K.-D. Lang, & H.-D. Ngo, *MDPI: Micromachines*, 12(11), 1429(2021); doi: 10.3390/mi12111429

[4] J. Ma, Y.L. Zhou, X. Bai, K. Chen, & B.O. Guan, *Nanoscale*, 11, 15821-1582 (2019); doi: 10.1039/C9NR04274A

[5] D.S. Li, X.H. Le, J.T. Pang, J.A. Xie, *In Processings of the IEEE 32nd international Conference on Micro Electro Mechanical System (MEMS)*, Seoul, Korea, pp.500-503(2019) 11, 15821-1582 (2019); doi: 10.1109/MEMSYS.2019.8870833

[6] J. Titze, M. Bäuscher, P. Mackowiak, M. Schiffer, K. Höppner, N. Grabbert, M. Schneider-Ramelow, J. Bickel, O. Pohl & H.-D. Ngo, *MDPI: The 1st International Electronic Conference on Chemical Sensors and Analytical Chemistry*, 10439(1-6), (2021); doi: 10.3390/CSAC2021-10439

[7] A. Stolarczyk, T. Jarosz, & M. Procek, *MDPI: Sensors*, 19(5), (2019); doi: 10.3390/s19051098

[8] J. Jaiswal, A. Das, V. Chetry, S. Kumar, & R. Chandra, *Sensors and Actuators B: Chemical*, 359, 131552 (2022); doi:10.1016/j.snb.2022.131552

[9] R. Kumar, S. Malik, & B.R. Mehta, *Sensors and Actuators B: Chemical*, 209, 919-926 (2015); doi:10.1016/j.snb.2014.12.037

[10] H.Z. Ma, Y.J. Zou, S. Zhang, L. Liu, J. Yu, & Y.M. Fan, *Carbohydrate Polymers*, 291,119544 (2022); doi:10.1016/j.carbpol.2022.119544

[11] S. Charan, N. Sharma, A. Kumawat, S. Mathur, A.K. Vishwkarma, & S. Shrivastava, *International Journal of Hydrogen Energy*, 48(96),38118-38124 (2023); doi:10.1016/j.ijhydene.2022.12.177

[12] Y. Pak, S.M. Kim, H.Jeong, C.G. Kang, J.S. Pak, H. Song, R. Lee, N.S. Myoung, B.H. Lee, S. Seo, J.T. Kim, & G.Y. Jung, *ACS Appl Mater Interfaces*, 6(15),13293-8 (2014); doi:10.1021/am503105s

[13] S. Raghu, P.N. Santhosh, S. Ramaprabhu, *International Journal of Hydrogen Energy*, 41(45),20779-20786 (2016); doi: 10.1016/j.ijhydene.2016.09.002

[14] D.H. Shin, J.S. Lee, J. Jun, J.H. An, S.G. Kim, K.H. Cho, & J. Jang, *Scientific Reports*, 5(1), 1-11, (2015); doi: 10.1038/srep12294

[15] X.H. Tang, P.A. Haddad, N. Mager, X. Geng, N. Reckingers, S. Hermans, M. Debliquy, & J.P. Raskin, *Scientific Reports*, 9(1), 3653, (2019); doi: 10.1038/s41598-40257-7